Final-state screening and chemical shifts in photoelectron spectroscopy

B. W. Veal and A. P. Paulikas
Materials Science and Technology Division, Argonne National Laboratory, Argonne, Illinois 60439
(Received 23 July 1984)

Photoelectron spectroscopic measurements of core-electron levels in cations of transition-series insulators commonly show "satellite" features in the vicinity of the "main" photoelectron peaks. In this paper, the relationship between main lines and adjacent satellites is systematically examined for $3d$-series insulators. The spectral features are interpreted using a relaxation model that allows for the possibility of different final-state screening conditions of the photoinduced hole. Systematic trends are examined by employing atomic calculations and utilizing transition-state theory to calculate electron removal energies for atoms in appropriately simulated chemical environments. It is demonstrated that the main-line and satellite energies are both dependent on the cation charge environment but with different degrees of sensitivity. The consequence is that sensitivity to chemical change can be monitored in the observed main-line to satellite separation. Model predictions are tested by monitoring the dependence of the satellite separations on the cation valence state and on the electronegativity of both cations and ligated anions. Systematic tests are applied to $3d$-series insulators but more general applicability of the relaxation model is also discussed.

I. INTRODUCTION

It was established by Siegbahn and co-workers[1] that sharp peaks could be observed in energy-analyzed photoemitted electrons following irradiation of a solid sample by monochromatic x rays. These peaks correspond to the binding energies (BE) of occupied core-electron levels. Since those binding energies are sensitive to local-charge environments, it was expected that the binding energies and hence the x-ray photoelectron spectroscopy (XPS) peaks would shift significantly as the chemical environment (e.g., valence state) was altered. Chemical shifts are, of course, observed in XPS lines, sometimes with dramatic effect. For example, chemical shifts between XPS core levels for carbon atoms in different chemical environments are sometimes 10 eV or more.[1-3] Often, however, the chemical shifts are disappointingly small (2 eV or less) even when valence changes, involving significant charge redistributions, occur. It has, of course, long been recognized that the XPS peaks do not directly measure local ground-state charge environments. Because relaxations or secondary excitations are always associated with core-hole production, it is generally difficult to determine the precise correspondence between XPS peaks and ground-state properties.

Complicating the interpretation of chemical shifts is the tendency, for cations in transition-element compounds (i.e., $3d$, $4d$, and $5d$,[4-30] lanthanides,[31-37] and actinides[38-44]) to show satellite features in the vicinity of XPS core lines. Typically, a single, relatively strong "satellite" will appear at the high-binding-energy side of the "main line." The low-binding-energy main line is almost universally the more intense one. The satellites appear within ~ 1 Ry of the main line and tend to be associated with all core levels of the cation. These satellites are generally called "shakeup" peaks.

Spectral complexity can also be introduced at core levels by the exchange interaction between the core hole and the localized electrons in an unfilled outer shell[45] (multiplet splittings). Splittings can be large at those shallow core levels where the radial wave function is comparable to the radial function of the outer-shell local electrons. Structure may sometimes be introduced at deeper core levels, also. However, such effects appear to be generally small at the deep levels of $3d$ insulators, serving to provide some apparent line broadening or weak substructure.[46]

It is generally agreed that photoemission peaks (disregarding peaks resulting from extrinsic loss processes) measure the energy difference between the ground state of the sample and (suitably metastable) final states of the ionized sample. Inevitably, creation of a deep core hole will cause readjustment of many electrons in the system including all "spectator" levels of the ion itself. All molecular orbitals to which outer electrons of the ion contribute will also be perturbed. Thus, unavoidably, a complex multielectron response of the ion and its local environment will occur in association with photoejection. If one perceives the outgoing photoelectron as being sensitive only to those final metastable states of a many-electron system (without giving consideration to ongoing temporal processes except perhaps for their effect on linewidths), then one typically seeks to discover, and to characterize as completely as possible, those final metastable ion states that exist in the company of the photoinduced core hole. Of course, the hope is that information relating to the ground-state chemical condition can also be inferred.

The substantial body of literature on the subject of satellite structure contains speculations about the direction of charge flow following creation of a core hole and possible configuration changes that might provide an identification of those final excited states that correspond to observed XPS peaks. The descriptive terms shakeup and shakedown have evolved, apparently to designate an exci-

tation or a relaxation (processes usually defined in relation to the energy state corresponding to the most intense "main" XPS line). There appears to be no clear distinction between these terms except to indicate that one final ion state is either higher or lower in energy than a designated (e.g., main line) reference state.

In the recent literature, a growing body of evidence points to the importance of considering relaxation phenomena, following core-level photoejection, to account for both the main-line and satellite features in insulating compounds.[24,47,48] Varying levels of relaxation of the photoinduced ion (providing differing screening or polarization conditions of the core hole) are thought to account for the observed XPS peaks. This view was advocated by the authors in a study of $3s$ line shapes in transition-metal fluorides.[49] The $3s$ line shapes were explained by considering two final-state screening conditions. The screening state specifies a $3d$ population which, in turn, determines the amount of exchange splitting at the $3s$ level. The combination of two screening states, each with a different $3d$ population, and the associated exchange splittings successfully predicted the observed line shapes. It was, furthermore, argued that different final-state conditions, reached in a relaxation response to the photoinduced hole, may account for the preponderance of structure that appears in cation deep core-level photoemission spectra of ionic compounds.

Final-state relaxation and core-hole screening have been considered by numerous other researches studying photoemission spectra of metals and of adsorbates on metallic substrates.[50–59] However, the screening arguments generally are not offered for insulators. Some authors specifically exclude the possibility that screening $3d$ electrons can locally reside at the cation site in insulators.[51,59]

In this paper we examine the relationship of the different final-state conditions to XPS core-level binding energies observed for elements in different chemical environments. The discussion will primarily focus on the energy separations between main-line and satellite structures in insulating compounds of $3d$ transition elements and on the chemical sensitivity of these relative energies. Emphasis will, therefore, be placed on extracting chemical information from measurements of the internal electron-level structure.

II. THE SCREENING MODEL

A. Description

In the presence of a core hole, unfilled eigenlevels associated with the ion are pulled down (to higher binding energy) relative to the eigenlevels of the atom in its ground-state environment. One of these pulled-down levels could become populated to locally charge-compensate the core hole.[60] This compensation process represents a partial deexcitation of the system and the kinetic energy of the outgoing electron will correspondingly be increased by the amount of this deexcitation energy. This process, of course, translates to a corresponding decrease in the apparent binding energy of the XPS line. Thus, if both the bare (unrelaxed) hole and the screened hole could be observed, then the screened condition would appear in XPS at the low-binding-energy side, with the bare hole at the higher binding energy.

Figure 1 illustrates the relaxation process which leads to the final-state screening or polarization conditions. Here we schematically represent the local density of states for cations and ligands in the vicinity of the Fermi level (E_F) for a (fully ionized) transition-metal insulator that contains unfilled $3d$ levels. In the presence of the core hole, outer levels will be pulled down (in the case of a free ion or unscreened hole, by about a rydberg). This is generally a sufficiently large shift in the level structure so that the extended $4s$-p orbitals will energetically overlap the ligand $2p$ orbitals. Furthermore, both the cation s-p's and the ligand $2p$'s are substantially extended spatially so these levels strongly overlap, both in energy and in space. This strong orbital overlap provides favorable conditions for (partial) population of the cation s-p screening orbitals (from the distributed ligand $2p$'s) in response to the sudden creation of a photohole (a resultant polarization condition). Although partial charge compensation might be accomplished by this "nonlocal" s-p orbital occupancy, the "ground-state" ion (i.e., the fully relaxed ion) is realized with occupation of a "local screening" orbital that is predominately $3d$ in character[61] (see Sec. III). Electrons in the nonlocal screening orbitals may reside in those states for times well in excess of 10^{-16} sec (a typical "photoemission lifetime" as determined by observed XPS linewidths). Thus, both final-state conditions are likely to be sufficiently metastable so that both will produce sharp features in the XPS spectrum. (Spectral complexity could be increased if time-dependent orbital repopulation was significant during the time frame of the photoemission measurement.[62]) We shall see that the radial extent of the

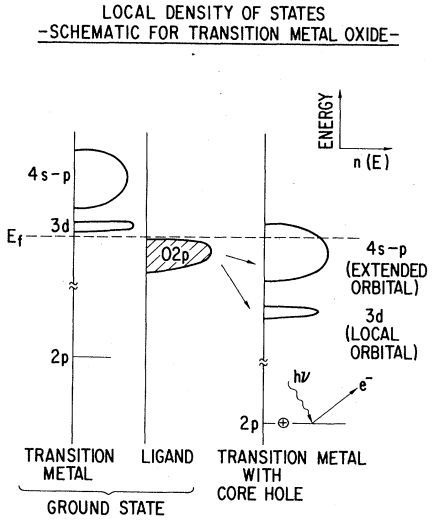

FIG. 1. A schematic representation of the local density of states at the cation and ligand sites in a (fully chemically ionized) transition metal oxide. Upon creation of a cation core hole by photoemission, other "spectator" levels of the cation are pulled down (to higher binding energy). It is then energetically favorable for charge from neighboring (ligand) atoms to flow toward the ion to screen the core hole. The observed XPS binding energy for removal of a core electron will depend upon the radial distribution of the screening charge.

screening orbitals has a strong influence on the excitation energies required to reach the different final screened states. Relative amplitudes of the screening states depend on the initial population probabilities and possibly upon temporal "trickle-down" processes wherein screening electrons fall from the nonlocal states to the less excited locally screened state.

The traditional view of photoemission in insulators is that relaxation accompanying core-hole production occurs via an electronic polarization response in the solid.[63] Except perhaps for the occupied atomiclike orbitals, all outer electrons of the system are in chemically filled shells. Thus no free-electron charge (as in metals) is available to screen a core hole. It is argued that the binding energy of a core photoemission event will, nonetheless, be reduced by the polarization energy, a form of extra-atomic relaxation. Estimates of relaxation energies accompanying core-electron photoejection have, for example, been reported for alkali and zinc halides.[52,64] For transition-metal insulators, a similar kind of charge-compensation response can occur (nonlocal screening). However, we have argued that charge compensation of a photohole can also occur by occupation of a localized (d-electron) cation orbital. This electron charge is drawn from the hybridized ligand-p band.

Charge compensation of the core hole by means of these different processes represent two very different final-state conditions. For d-electron compensation (local screening), an excitonlike impurity (that is approximately charge neutralized) appears at the photoionized site. No significant charge imbalance is now discernable at the screened atom. The solid has, nonetheless, been deprived of one electron. The hole must, therefore, redistribute in a bubble of substantial spatial extent about the screened hole. Thus, local charge compensation of the photohole should result in a spatially extended polarization cloud with small internal field gradients, very similar to the physical condition that results when an electron is directly removed from the ligand p band. (Coulomb repulsion demands that the hole will be dispersed.) In contrast, a polarization response which does not involve a charge-compensating $3d$ electron (nonlocal screening) leaves the system with a strong local Coulomb potential which must be compensated by polarization of the atoms in closely neighboring shells. Thus a "local screening state" results in an extended polarization cloud while "nonlocal screening" is associated with a more compact polarization cloud.

In general, we expect that, for transition-element insulators, two final states will be observable. One state corresponds to a fully relaxed (locally screened) condition involving occupancy of a screening transition-series electron level. The second (nonlocal screening) state corresponds to a many-electron relaxed final state of the ion that excludes occupancy of the localized transition-series (e.g., $3d$) electron[65] level.

B. Relationship to shakeup and shakedown

The seemingly contradictory processes of shakeup (an implied excitation) and shakedown (an implied relaxation) as mechanisms to explain cation satellite structure have led to substantial confusion. When a core hole is created, the system relaxes, both intra-atomically and extra-atomically, with a complex collective response, toward the ground state of the ion. Metastable intermediate states (semirelaxed) may be encountered by the ion on its way toward complete relaxation. Thus, multiple peaks could be observed. (In our view, the preponderance of multiple-peak structure that appears at XPS core levels within ~ 1 Ry of the main line can be accounted for with this simple relaxation model.) Thus the terms shakeup and shakedown are consistent with the model considered here if we regard shakedown as a process by which the system adjusts to the sudden presence of the core hole in order to reach the (fully or partially) relaxed final metastable states and if we regard shakeup as a term to designate excitations of the final ion state *measured with respect to the fully relaxed ion.*

If a photoinduced core hole is suitably long lived and the system response to creation of the deep hole is suitably fast, then XPS will monitor the fully relaxed (ground state) of the ion with its deep core hole. The corresponding XPS peak will, of course, occur at the lowest possible binding energy for this hole state. Any other XPS peak associated with the core hole will represent an excitation with respect to the fully relaxed ion state. The kinetic energy of the outgoing photoelectron from any higher binding energy peaks will be degraded relative to the electrons associated with the fully relaxed peak.

Reference 66 reviews the variety of assignments that have been reported to account for satellites in transition-metal complexes. A ligand-to-metal $3d$ charge-transfer shakeup process appears to be the most generally accepted explanation for the dominant satellite peaks in transition-element insulators. However, excitation assignments are usually made without first characterizing the fully relaxed hole state. Thus, in our view, this methodology is often inappropriate. The energetics of the final state require that charge flows (or relaxes) toward the cation to charge-compensate the core hole. Thus a "charge-transfer relaxation" would always be a process associated with core-level photoejection. Furthermore, the ligand- (band orbital) to-cation $3d$ transition constitutes a process whereby the ion is moving toward a *highly relaxed* condition. (We have argued that this process produces the low-binding-energy *main* XPS line.) Thus, a ligand-to-$3d$ *shakeup* assignment for the *satellite* would, in general, not appear to be appropriate.

Some authors are careful to point out that the intense, lowest-binding-energy XPS line must correspond to a fully relaxed condition of the ion. However, if charge-transfer shakeup is then invoked to explain the satellite, are we to understand that a charge-transfer excitation *from the fully relaxed state* has occurred? In our view, this would be an acceptable perception of shakeup but it is a description that requires a clear understanding of the fully relaxed state (and would suggest that the satellite results from a $3d$-to-ligand charge transfer.)

In some cases, the final state of the ion may be left sufficiently excited that one could not reasonably view it as having been reached in a net relaxation process.[67] In gen-

eral, however, this distinction has little value since the point where a "net" relaxation or excitation occurs cannot be precisely defined.

III. INSIGHTS FROM ATOMIC CALCULATIONS

We shall make extensive use of a relativistic local-density atomic code[68] to calculate eigenvalues and transition energies for groups of atoms or ions systematically configured to simulate chemical changes. For example, Fig. 2 shows eigenvalues for "atomic" chromium with the outer electron configurations $(3d^5 4p^1)$, $(3d^4 4p^2)$, $(3d^3 4p^3)$, and $(3d^2 4p^4)$. The replacement of a localized $3d$ electron with a more extended $4p$ electron simulates the process of increased chemical ionization (e.g., increased valence state) at the cation site. Increasing the cation valence (usually) means that charge is drawn from the immediate vicinity of the cation and is redeposited on neighboring ligand atoms which closely surround the cation. The net effect is qualitatively much like the process of converting the local $3d$'s into the extended $4p$'s, thus leaving a more positive potential at the cation site. A properly chosen set of atomic orbitals should reasonably approximate the spherical average of the radial charge distribution centered at the cation site. To represent a change in cation valence will, of course, require a different orbital set.

The eigenvalues of spectator levels (Fig. 2) move down as the outer electron charge is pushed further from the cation center. The more localized the eigenfunctions of these spectator levels are, the more rapidly the levels move down (although deep core levels all move at very nearly the same rate since their charge is essentially all interior to the outer orbitals where "chemical" effects occur).

Figure 2 indicates that substantial shifts in measured binding energies of cation core levels might be expected as the ligand electronegativity or cation valence is altered. However, Fig. 2 represents ground-state conditions for chemically different environments, and spectroscopies never directly measure those ground states. In XPS the total energy difference between the ground state and some final ion state is measured.

For atoms, the excitation energy added to promote the transition between a specified ground state and a specified final state can be obtained from transition-state (TS) calculations using the Dirac-Slater local-density formalism.[69] Thus the energetics of a simulated photoemission process can be examined using transition-state calculations. With the local-density code, excitation energies for (unscreened) ionization are calculated by removing $\frac{1}{2}$ of an electron from the core state. The excitation energy is then given by the (negative of the) eigenvalue of the fractionally occupied core level.

Figure 3 shows eigenvalues (upper dotted lines) at the $2p_{3/2}$, $3p_{3/2}$, and $3d_{3/2}$ core levels for the ground state of the "Cr atom" with configuration $(3d^3 4p^3)$. Also shown as (lower) dotted lines are eigenvalues for the ionized atom: in Fig. 3(a), for a hole at the $2p_{3/2}$ level; in Fig. 3(b), for a hole at the $3d_{3/2}$ level; and in Fig. 3(c) for a hole at $3p_{3/2}$. We note that the electron-removal energy (i.e., the transition-state energy labeled unscreened ion in Fig. 3) is approximately midway between the ground-state and ion eigenvalues with the eigenvalues, in general, being

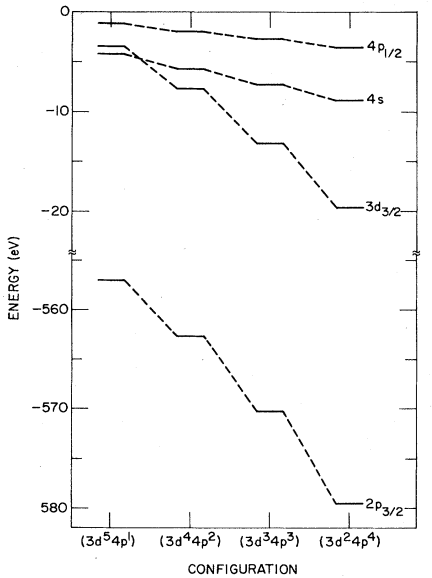

FIG. 2. Ground-state eigenvalues from atomic calculations of several configurations of $Cr(3d^n 4p^{6-n})$. These configurations simulate varying levels of chemical ionization of the chromium atom. Replacement of a localized $3d$ electron with a radially extended $4p$ places charge more remotely from the ion center and thus corresponds to an increased level of chemical ionization. Localized levels (including $2p$'s and $3d$'s) move rapidly, in near unison, to higher binding energy as ionization is increased. Extended levels respond more slowly to chemical changes.

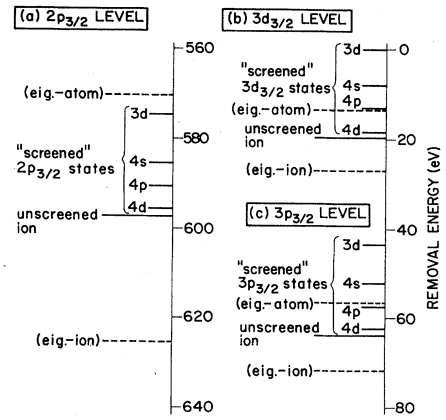

FIG. 3. Calculated electron-removal energies at the $2p_{3/2}$, $3p_{3/2}$, and $3d_{3/2}$ levels for $Cr(3d^3 4p^3)$. The levels marked "unscreened" are transition-state (TS) calculations for electron removal from the isolated $Cr(3d^3 4p^3)$ "atom." These TS results fall approximately midway between the calculated eigenvalues for the ground state (dashed levels labeled eig.-atom) and calculated eigenvalues for the hole state (dashed levels labeled eig.-ion). Levels labeled "screened states" are TS calculations (electron-removal energies) of simulated screening conditions of the core-hole state. These levels represent the energy difference (excitation energy) between the ground state and the final state that contains a core hole and an occupied outer (screening) electron level (designated $3d$, $4s$, etc.).

very different from ionization (TS) energies. The eigenvalues represent the initial-state atom and final-state ion; the transition state represents the ionization energy required to convert the atom from its initial state to its final state (including the energy associated with intra-atomic relaxation of all spectator levels[69]). We shall see that TS calculations, particularly when screening conditions are properly considered, can provide very accurate determinations of XPS core-level energies (see Sec. V E).

To simulate photoemission involving the screening conditions described in Sec. II, we remove $\frac{1}{2}$ of an electron from the core level and add $\frac{1}{2}$ of an electron into a screening orbital. For example, if screening is local (i.e., $3d$), the excitation energy $E_{\rm exc}$ for Cr $2p_{3/2}$ photoemission from a (fictitious) solid containing chromium ions in an environment locally represented by the configuration $(3d^3 4p^3)$ would be $E_{\rm exc} = -E_{2p_{3/2}} + E_{3d_{3/2}}$, where $E_{2p_{3/2}}$ and $E_{3d_{3/2}}$ are eigenvalues from the atomic calculation of $1s^2 2s^2 2p_{1/2}^2 2p_{3/2}^{3.5} 3s^2 3p^6 (3d^{3.5} 4p^3)$. Alternately, nonlocal screening of the photohole would be calculated by placing $\frac{1}{2}$ of an extended-state electron (e.g., a $4s$ or $4p$) into the screening orbital. For the configuration $(3d^3 4p^3)$, the energetics of the bare ionization process and various screening conditions ($3d$, $4s$, $4p$, etc.) are shown in Fig. 3. We see that the electron-removal energy is greatest for the unscreened final state and becomes progressively less as the screening orbital becomes more localized. The solid lines shown in Figs. 3(a), 3(b), and 3(c) for the various screening states represent the multipeak (satellite) structure that one would expect to observe for a "free chromium atom" of ground-state configuration $(3d^3 4p^3)$ if the atom could acquire the needed screening electrons (from a common source) during excitation. Note that the difference in removal energies for the various screened states is comparable for ionization at the $2p$, $3p$, and $3d$ levels.

Important insights for interpreting XPS spectra are also gained if one appreciates that the outer-electron states of a (fully relaxed) ion of atomic number Z that has a deep core hole and a compensating (screening) outer electron are well approximated by the ground state of the neutral $Z+1$ atom. That is, to the outer electrons, a Coulomb-potential change produced by adding a sufficiently localized core hole is indistinguishable from the potential change produced by adding a proton to the nucleus.[70] To illustrate, we compare, in Fig. 4, outer-electron eigenvalues for ground-state atomic iron $\mathrm{Fe}(3d^6 4s^2)$ with corresponding eigenvalues for (locally screened) $\mathrm{Fe}(1s^1 3d^7 4s^2)$ containing a $1s$ core hole and a compensating $3d$, and with eigenvalues for ground state $\mathrm{Co}(3d^7 4s^2)$, the $Z+1$ analog of the excited Fe atom. We see that, for levels outside (and including) the $2p$ shell, only minor differences occur between corresponding core-level energies of the highly excited Fe atom and the ground-state Co atom (although $1s$ eigenvalues differ by more than 300 eV). An application of the $Z+1$ model to predict satellite structure will be discussed in Sec. V D.

Clearly, the excitation energies, like the eigenvalues (Fig. 2), must depend on the ground-state charge (or "chemical") condition. The excitation (TS) energies at the $2p_{3/2}$ level for the ground-state chemical ionization conditions illustrated in Fig. 2 are shown in Fig. 5. Here we present excitation energies for the bare ionization (dashed line) and for local ($3d$) and nonlocal ($4s$,$4p$) screening of the core hole. Recall (in these simulated chemical ioniza-

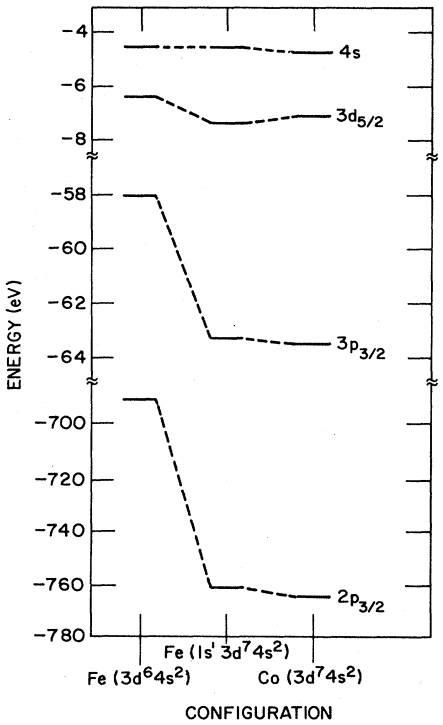

FIG. 4. Calculated eigenvalues for $\mathrm{Fe}(3d^6 4s^2)$ and for $\mathrm{Co}(3d^7 4s^2)$ compared with eigenvalues for $\mathrm{Fe}(1s^1 3d^7 4s^2)$. The comparison of $\mathrm{Fe}(1s^1 3d^7 4s^2)$ and $\mathrm{Co}(1s^2 3d^7 4s^2)$ demonstrates that a deep core hole (here at the Fe $1s$ level) has a comparable effect on the outer electron level structure as does a proton added to the nucleus. Thus, screening of a deep core hole may be approximated by the level structure of $Z+1$ impurity.

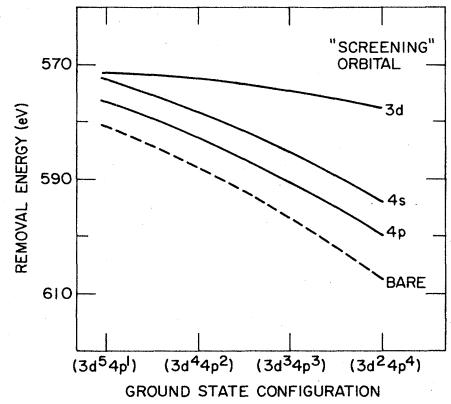

FIG. 5. Dependence of electron-removal energies (TS calculations) on simulated chemical ionization for the Cr $2p_{3/2}$ level. The dashed line represents simple electron removal while lines labeled $3d$,$4s$,$4p$ are energy differences between the ground state (noted on the abscissa) and the final state that contains a core hole and an occupied $3d$, $4s$, or $4p$ (screening) electron level. These results show that, for $3d$ screened final states, removal energies are very insensitive to ground-state chemical changes.

tions) that the radial charge distribution at the metal site is shifted outward as $3d$ electrons are replaced by $4p$'s thus corresponding to an increase in valence. As the valence state increases, the transition-state energy for the unscreened hole moves repaidly to higher binding energy. However, the TS energy for the locally screened level shows only a small shift as the valence is changed. *This result explains why observed XPS core-level shifts of cations can be so disappointingly small.* Even if a large change is made in the valence state of a cation, only a very small chemical shift will be observed in the intense XPS line if the core hole is always screened by a localized electron.

Local screening shows little chemical sensitivity because the transition from ground state to screened final state is essentially equivalent to an excitation from a (localized) core level to a localized outer level. We saw in Fig. 2 that localized levels move in near unison as the valence state is altered. The transition energy from the core level to the local outer level (unlike transitions to the extended outer level) is thus relatively independent of chemistry. Figure 5 has shown that the locally screened cation XPS peaks are very insensitive to chemical changes. However, substantially stronger chemical sensitivity is expected if the screening is nonlocal. Thus the relative separation between XPS main line and satellite (locally and nonlocally screened XPS final states) should be sensitive to variations in the local cation charge environment. Thus we see the possibility that chemical changes can be monitored by measuring the relative separations between the main line and satellite.[71] Figure 5 suggests that the satellite separation is closely related to the ground-state potential at the cation site. The greater the local positive charge at the cation site, the greater is the expected satellite separation.

For $3d$ insulators, the low-lying nonlocal screening state will normally consist of $4s$ or hybridized $4s$-$4p$ band states that contain some admixture of $3d$ and ligand orbitals. If the character of the nonlocal screening state can be estimated, then one can use the measured satellite separation to determine a configuration for the atomic calculation that provides an estimate of the ground-state potential at the cation site (e.g., see Fig. 5). To demonstrate the validity and general utility of the screening model for interpreting XPS spectra, we systematically examine, in the next section, experimental core-level spectra for simple compounds observed under varying chemical conditions and compare observed results with the model predictions.

IV. EXPERIMENTAL

Spectra displayed in this paper were recorded using a Hewlett-Packard model No. 5950A photoelectron spectrometer. A monochromatized Al $K\alpha$ x-ray source provided incident x-ray radiation at 1486.6 eV. The overall instrument resolution was ~ 0.7 eV. A thermal electron source, with adjustable filament temperature and accelerating potential, was used to flood the sample with electrons to minimize sample charging. For each sample, flood gun parameters were tuned to minimize spectral broadening. Some of the samples were powder compacts held onto a gold-coated substrate with an indium interface layer. Other samples were cut from ingots prepared by melting or sintering. These samples were cleaved or scraped *in situ* with an alumina rod to expose a clean surface.

For this study, our intent was to choose relatively simple and stable compounds which provide a range of chemical properties (e.g., variable valence state and cation-ligand bond strength), while minimizing experimental difficulties. We argue that satellite energies may quite generally be used to discern chemical properties of transition-element cations in different environments. However, we have not chosen to test the model predictions by extensively utilizing measurements reported in the literature. In some cases, satellites are relatively weak, and interfering structures from extrinsic loss processes can make data interpretation difficult (e.g., see Sec. V D). For these reasons, tabulated values of satellite energies are particularly inappropriate. Also, *in situ* sample reduction problems (particularly for samples containing high valence cations and heavier halides), inadequate valence-state isolation (frequently a problem with commercially obtained samples), and surface oxide contamination can provide misleading results. For some compounds, satellite energies reported in the literature vary widely. Thus for this study we chose systems which, in general, show strong satellites. Surface oxides and *in situ* reduction tendencies were carefully monitored to ensure that their influence on satellite positions was minimal.

The iron chloride samples were very hygroscopic. Since spectral detail was sought at the weak Fe $3s$ levels, both hydrous and anhydrous forms were measured to check for spectral distortion resulting from residual water (or oxygen) contamination. In the spectrometer, the hydrates showed severe outgassing tendencies, probably associated with dehydration. The anhydrous $FeCl_2$ sample was a single-crystal ingot which was loaded into the spectrometer from a nitrogen-gas atmosphere. The sample was mounted with Torr-Seal epoxy (from Varian, Inc.) and was cleaved just prior to insertion. No oxygen or carbon contamination was observed on the cleaved surface. A spectrum taken three days after initial loading into the vacuum system showed the presence of both carbon and nitrogen, but no apparent oxygen. No discernable differences were noted between the (Fe $2p$ or Fe $3s$) spectra of ingot $FeCl_2$ and powder $FeCl_2 \cdot 4H_2O$.

For the $FeCl_3$ samples, only powder specimens were available. For the hydrous material, severe outgassing initially occurred in the spectrometer, probably resulting in a significantly dehydrated sample. The anhydrous $FeCl_3$ sample was loaded from a nitrogen-gas atmosphere. The oxygen XPS signal was reduced by about a factor of 2 relative to the hydrate, but it was not eliminated. Again, spectra for the "anhydrous" $FeCl_3$ and the (dehydrated) $FeCl_3 \cdot 6H_2O$ samples were very similar. The presence of residual oxygen suggests that the sample surface is rather poorly characterized and may contain oxyhalide(s). However, the Fe^{3+} state is apparently preserved in a predominately Cl environment. Spectral distortions at the Fe levels (at our level of signal-to-noise ratio) introduced by the

TABLE I. Satellite energy measured relative to cation $2p_{3/2}$ level (Sc data are from Ref. 25).

		E_{sat} (eV)			E_{sat} (eV)
Fe^{2+}			Fe^{3+}		
	FeF_2	6.3		FeF_3	9.1
	$FeAl_2O_4$	5.7		Fe_2O_3	8.2
	$FeCl_2$	5.4		$FeCl_3$	7.0
	$FeBr_2$	4.8			
			Zr^{4+}		
Sc^{3+}				ZrF_4	14.2
	ScF_3	12.3		ZrO_2	13.0
	Sc_2O_3	11.4		$ZrCl_4$	11.7
	$ScCl_3$	9.5			
	$ScBr_3$	8.4	Ti^{4+}		
	ScI_3	7.4		TiF_4	14.4
	Sc_2S_3	9		TiO_2	13.3

presence of oxygen appear to be small.

In general, the trends reported here are confirmed by measurements of satellite separations reported elsewhere in the literature. Independent measurements of satellite separations for the compounds reported in Fig. 10 appear in Refs. 4, 9, 13, 17, and 25. Data for the scandium compounds are from Ref. 25. Agreement between the cited measurements of satellite separations and our own measurements is usually within 3%. For the compounds of Fig. 10, the satellite energies (measured relative to the $2p_{3/2}$ peak) are listed in Table I. The binding-energy reference scales used in Figs. 8, 11–16, and 18 were taken from the $2p_{3/2}$ levels of appropriate compounds listed in Ref. 2.

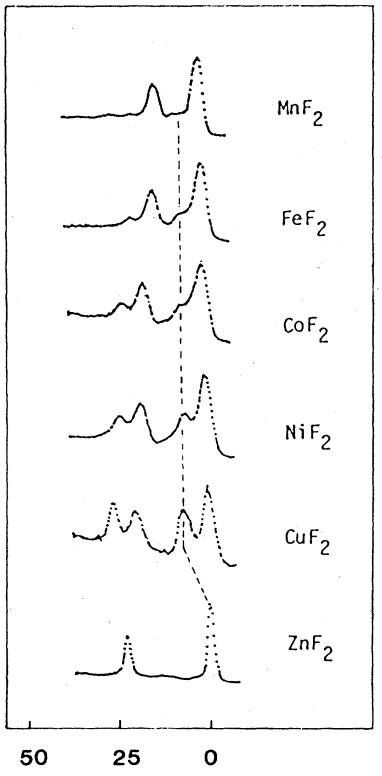

FIG. 6. XPS spectra for spin-orbit-split $2p_{1/2}$ and $2p_{3/2}$ levels in a series of transition-element difluorides showing main-line and satellite features. Spectra are presented with the intense (main lines) of the $2p_{3/2}$ levels in alignment; the abscissa records the binding energy in relation to the aligned main lines. For the compounds of Mn-Cu, the main line corresponds to a locally screened (d^{n+1}) final state with the satellite resulting from nonlocal screening (d^n final state). Since $3d$ screening cannot occur in ZnF_2, no satellites appear and the peaks correspond to nonlocally screened final states. The nonlocal screening state for $2p_{3/2}$ emission is indicated with the dashed line.

V. DISCUSSION

A. Typical core-level spectra and satellites

Figure 6 shows XPS spectra of the $2p$ levels in a series of $3d$ transition-metal difluorides (also see Ref. 4). Spectra are presented with the intense $2p_{3/2}$ peaks in alignment. Except for ZnF_2, satellites appear adjacent to the spin-orbit-split main lines. These satellite intensities systematically increase, relative to the main line, with cation atomic number. The systematic behavior of the spectral features for the Mn-Cu series of compounds illustrates that the local screening condition (low BE peak) is dominant, especially for MnF_2, where essentially no satellite structure is observed. For ZnF_2, which has no unfilled $3d$ levels, only the nonlocal screening condition is possible. Consequently, no satellite structure (really no main line) is observed except for weak plasmon peaks that also occur adjacent to the F $1s$ level.

The spectra of Fig. 6 show satellites at the $2p$ levels for divalent transition-metal fluorides where satellites con-

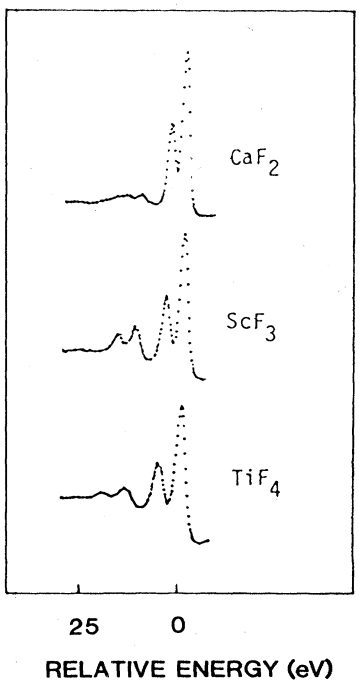

FIG. 7. XPS spectra for the spin-orbit-split $2p$ levels of CaF_2, ScF_3, and TiF_4 displayed with $2p_{3/2}$ levels in alignment. Strong satellites on the high-binding-energy side replicate the $2p$ doublet.

sistently appear about 6 eV removed from the intense lines. In Fig. 7 we show $2p$ spectra for $2+$, $3+$, and $4+$ cations of the compounds CaF_2, ScF_3, and TiF_4, respectively. These (chemically) fully ionized cations are from the low-Z side of the $3d$ transition series. For these compounds, satellites are significantly more separated from the main line (10—15 eV) than is the case for the difluorides. Here satellites replicate the main spin-orbit doublet without overlapping it. A significant feature of the satellite spectra in Figs. 6 and 7 is their relative simplicity. Satellite spectra associated with a given core line tend to be characterized by a single peak.

B. Cation valence

Figure 8(a) shows the Fe $2p$ levels for Fe^{2+} and Fe^{3+} ions in $FeCl_2$ and $FeCl_3$. Consistent with the predictions of Sec. III, we observe a small shift of the intense peak to higher binding energy as Fe valence is increased and a substantially larger shift of the satellite. The net effect is a small offset of the intense peak with an increasing separation between main line and satellite as the Fe valence is increased. The spectra of Fig. 8 are presented with the Cl $2p$ core levels in alignment. Since the local-charge environment at the Cl site might be different in the two compounds, this alignment procedure may not be entirely appropriate. In support of this procedure, however, the absolute binding energies of the Cl $2p$ lines for these two compounds, as reported in the literature,[2] are nearly equivalent. Also see Secs. V E and V I. While some uncertainty occurs in the relative positioning of the Fe^{2+} and Fe^{3+} peaks, the main-line—to—satellite separation clearly and dramatically increases with increase of Fe valence.

Also shown in Fig. 8(b) are the Fe $3s$ levels. These spectra are further complicated by a large exchange splitting, important when the $3s$ and $3d$ radial wave functions are comparable. Following the procedure cited in Ref. 49 (and using the same dependence of exchange splitting on $3d$ population), we calculate the $3s$ spectra. The calculated results are shown immediately beneath the measured spectra in Fig. 8(b). As in Ref. 49, the use of exchange splitting and multiple screening states appears to satisfactorily account for the observed line shapes. For the Fe^{2+} compound, the $3s$ spectrum is noticeably compressed because both the screening splitting and multiplet splitting are reduced relative to the Fe^{3+} compound.

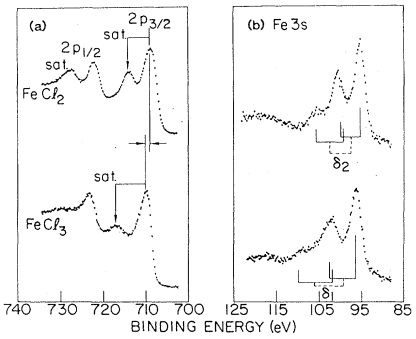

FIG. 8. (a) Spin-orbit-split $2p$-level spectra for Fe^{2+} and Fe^{3+} chlorides showing the low-binding-energy main lines and prominent satellites. Note that the larger separation between main line and satellite occurs for the higher valence cation. The main line of $FeCl_3$ also displays a small chemical shift to higher binding energy relative to the main line of $FeCl_2$. (b) Fe $3s$ levels in $FeCl_2$ and $FeCl_3$. Predicted exchange-split doublets offset by the screening splitting (δ_1 for Fe^{3+} and δ_2 for Fe^{2+}) are compared with measured $3s$ spectra (see text).

C. Ligand electronegativity: Effect on cation spectra

The potential at the cation site in a binary ionic compound is affected by the relative ability of neighboring ligands to withdraw charge from the metal atom. In general, as the ligand becomes more electronegative, we expect that the potential at the cation site will become more positive. (Of course, the cation potential can also be affected by the coordination number and relative orientations of neighboring ligands.)

The process of increasing ligand electronegativity is qualitatively represented in Fig. 5 by moving to the right on the abscissa (moving electron charge outward from the cation center). Thus, we expect to see an increase in the main-line—to—satellite separation as ligand electronegativity is increased. This expectation is confirmed in Fig. 9 where Fe $2p$ spectra are presented for the Fe^{3+} compounds FeF_3, Fe_2O_3, and $FeCl_3$.[72] Electronegativities (Pauling scale) for the ligands are 4.0, 3.5, and 3.0, respectively.[73] Other systematic measurements of transition-element systems in the literature which dramatically illustrate this correspondence between ligand electronegativity and satellite separation include a series of scandium compounds (ScF_3, $ScCl_3$, Sc_2O_3, $ScBr_3$, and ScI_3),[25] a corresponding (vapor-phase) Ti^{4+} series,[18] and a Mn^{2+} series.[26]

The satellite shift versus Pauling electronegativity is

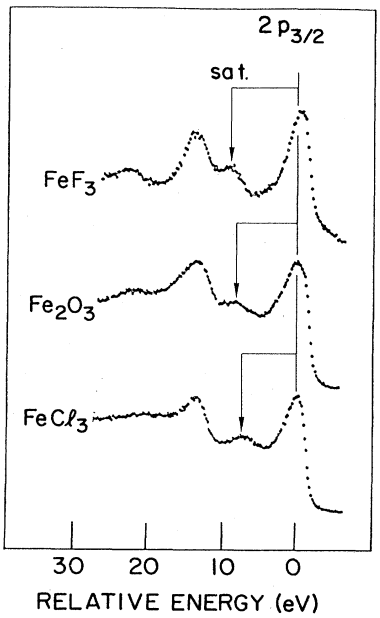

FIG. 9. XPS spectra for $2p$ levels in FeF_3, Fe_2O_3, and $FeCl_3$ shown with $2p_{3/2}$ levels aligned. Note that the satellite separation from the main line increases with ligand electronegativity.

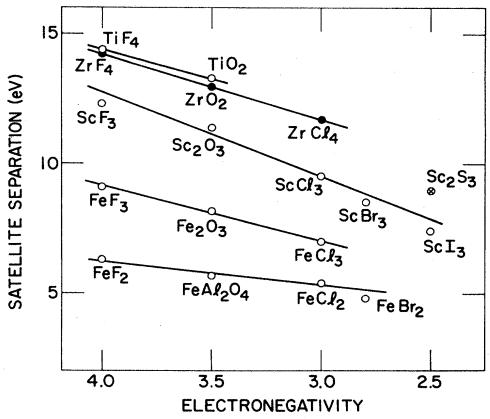

FIG. 10. Energy separations between main line and satellites in XPS spectra of cation $2p_{3/2}$ levels for a number of ionic compounds. Satellite separations are plotted versus ligand electronegativity (Pauling scale). The satellite energies show a systematic dependence on electronegativity and cation valence. As the charge environment at the cation site becomes more positive, the greater is the satellite separation.

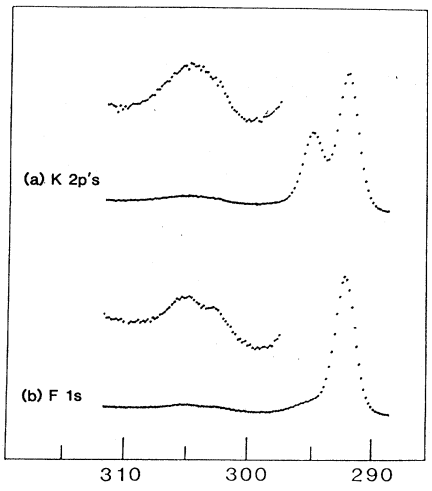

FIG. 11. (a) XPS spectra of K $2p$ levels in KF. Spectra on the high-binding-energy side, showing weak (apparently extrinsic) electron-loss processes, are blown up 8 times. (b) F $1s$ spectra of KF similarly displayed. The F $1s$ peak is aligned with the K $2p_{3/2}$ peak (energy scale pertains to the K $2p$ levels). Note the similar loss spectra following the F $1s$ and K $2p$ peaks.

recorded in Fig. 10 for a number of representative series of compounds. We note the following.

(1) In all of the series, the satellite shift increases as ligand electronegativity increases.

(2) The splitting increases with increasing cation valence as illustrated by the Fe^{2+} series and Fe^{3+} series.

(3) For highly electropositive cations (e.g., Sc^{3+}), the splitting is larger than for cations that have equivalent valence (e.g., Fe^{3+}) but are less electropositive.

D. $Z+1$ considerations: K^{1+} and Ca^{2+}

By applying the insights provided by the $Z+1$ analogy (see Sec. III) to the analysis of K^{1+} and Ca^{2+} spectra, another important test of the screening model is obtained. For K^{1+} (e.g., in KF) experiencing deep core photoionization, the $Z+1$ analogy suggests that the unscreened photoexcited ion is approximately equivalent to Ca^{2+}. For Ca, the ground-state atomic configuration is $3d^0 4s^2$. Furthermore, in solids, we expect Ca to have a very small (hybridized) $3d$ population (a fraction of one electron). Thus we expect that the ground-state screening condition of a deep hole in photoexcited K will be nonlocal. The unfilled $3d$ bands, lying well above E_F, are also highly delocalized and consequently will be hybridized with extended neighbor orbitals. Thus we expect that the K XPS core-level spectra will show no satellite structure attributable to local screening states. On the other hand, Ca^{2+} (e.g., in CaF_2), after having experienced deep core photoexcitation (but unscreened), is analogous to Sc^{3+}. The low-lying excited state should be predominantly $3d$. (Atomic scandium has the configuration $3d^1 4s^2$.) The low-binding-energy XPS peak at a Ca^{2+} core level thus should correspond to a locally screened state. Thus the final state closely approximates the Sc^{2+} ion which contains an occupied $3d$ level. If a suitably metastable nonlocal screening state is also available, both the main line and satellite should be observable (unlike the case for K).

In Fig. 11(a) we show the spin-orbit-split K $2p$ spectra of KF with the high-binding-energy side enlarged 8 times. In Fig. 11(b) the F $1s$ line is similarly displayed. Since a F $1s$ hole cannot be screened locally we expect to observe a single F $1s$ peak followed by extrinsic loss processes associated with an electron traversing the solid. In princi-

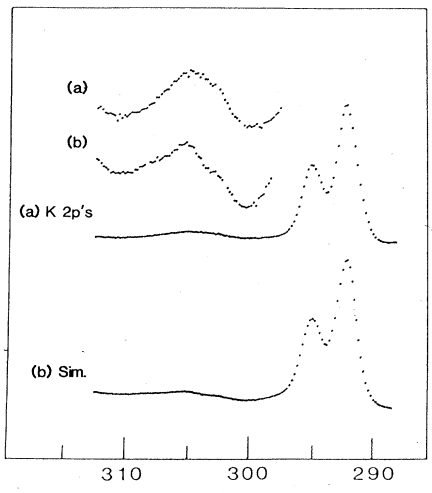

FIG. 12. To demonstrate that the background (loss) spectra following F $1s$ and K $2p$ spectra are of common origin, the K $2p$ loss region is simulated by superimposing two F $1s$ spectra properly scaled and offset to duplicate the spin-orbit components of the K $2p$'s. This offset-scaling procedure of the F $1s$ line nicely duplicates the K $2p$ loss region. Thus no K $2p$ satellite structure associated with different screening states of the $2p$ core hole can be discerned.

ple, shakeup excitations associated with the F 1s hole are also possible. However, KF is a wide-band-gap material so they should be quite energetic, probably outside the spectral range displayed in Fig. 11. (In fact, strong satellite structure, exclusive to the F levels, is observed in the alkali and alkaline earth halides at 25—30 eV from the main line.[74,75]) If the structure following the K 2p's and F 1s is predominately extrinsic, then we should be able to simulate the K 2p loss region by superimposing two F 1s spectra suitably scaled and offset to duplicate the spin-orbit components of the K 2p's. This simulation is presented in Fig. 12(b), where it is compared to the raw K 2p spectrum [Fig. 12(a)]. Both the magnitudes and shapes of the loss features in the simulated spectrum accurately reproduce the K loss spectrum. Surely no satellite peak, exclusive to the K line is apparent. For CaF_2, the Ca 2p and F 1s spectra are displayed in Fig. 13. Using the F 1s line and the procedure outlined above, a Ca 2p spectrum is simulated and displayed in Fig. 14(b). We see that a portion of the experimental Ca 2p loss region is nicely accounted for, but a residual doublet persists. If this residual doublet corresponds to a screening state, it should reproduce the intense spin-orbit doublet (with a possible linewidth difference). Thus we add to the simulated spectrum [Fig. 14(b)], the original Ca 2p spectrum (scaled by 0.04 and offset by 10.8 eV). This final composite is shown in Fig. 15 compared with the Ca 2p XPS data. We see that a remarkably accurate reproduction of the measured satellite spectrum is obtained. Thus we conclude that the satellite region consists of a single nonlocal screening state superimposed on an extrinsic loss background. The considerable difference in population of these two screening states apparently reflects differences in the overlap between the initial (ground) state and the two possible final-state wave functions. In any case, Figs. 11—15 demonstrate that multiple screening states are absent in KF but are clearly present in CaF_2, as predicted.

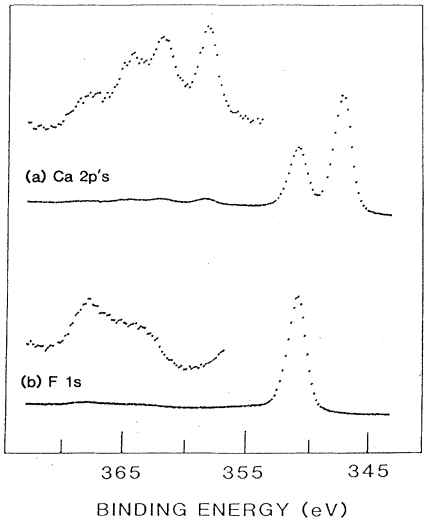

FIG. 13. (a) XPS spectra of Ca 2p levels in CaF_2. The high-binding-energy side is blown up 16 times. (b) F 1s spectra in CaF_2 similarly displayed (the energy scale pertains to the Ca core levels).

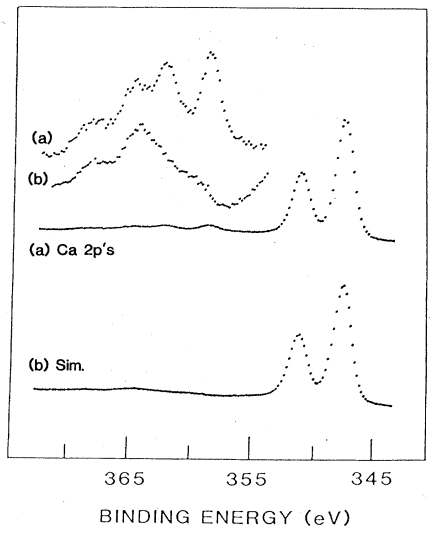

FIG. 14. (a) XPS spectra of Ca 2p levels in CaF_2. (b) Using two superimposed F 1s spectra [Fig. 13(b)] properly scaled and offset, the Ca 2p doublet is reproduced. Note that a portion of the high-binding-energy side is accurately reproduced but a residual doublet is not accounted for.

This analysis also demonstrates that considerable care must be exercised in interpreting the satellite features. The Ca 2p spectra (Fig. 13) consist of three sets of spin-orbit-split doublets, but one doublet is contributed by extrinsic loss features common to the core lines of both ca-

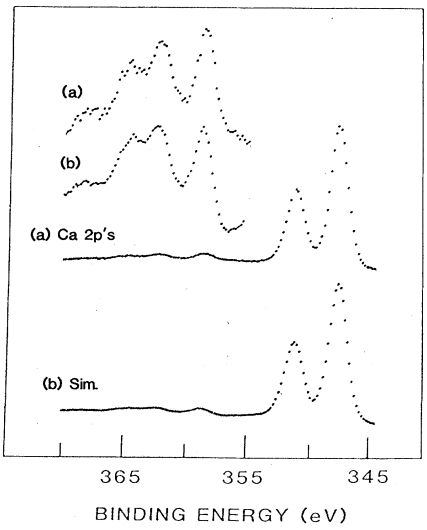

FIG. 15. (a) XPS spectra of Ca 2p spectra in CaF_2. (b) Ca 2p spectrum (scaled by 0.04 and offset by 10.8 eV) added to the simulation of spectrum (b), Fig. 14. The sequence of simulation steps for the Ca 2p spectra (Figs. 13—15) indicates that a single satellite spectrum intrinsic to the Ca 2p's is superimposed on an extrinsic spectrum whose origin is also common to the F 1s spectrum. These results support the view that the Ca 2p satellite region contains a nonlocally screened final state with the intense lines corresponding to a locally screened final state. KF, in contrast, does not show multiple screening states (see Figs. 11 and 12).

tion and ligand.

The fact that K and Ca ions show very different but predictable satellite structures provides strong evidence in support of the screening model. The Ca cation, even though it has no occupied $3d$ electrons, shows behavior which is typical of the cations in $3d$ transition-series insulators. The important common feature is that, when photoionized, the first unoccupied level is $3d$.

E. Chromium compounds

The local screening condition for photoexcitation from the outermost (partially filled) shell of localized levels (e.g., for photoemission from a $3d$ level of a first long series cation) assumes particular significance. The measurement of a $3d$ hole screened by an identical $3d$ means that the total energy difference (i.e., the transition-state energy) between the initial ground state and the final screened state is approximately zero (except for the energy required to move one electron across the work-function barrier and possible multiplet excitations which may appear in the spectra). This screened final state corresponds to the level appearing at $E=0$ in the simulation of Fig. 3(b). In the absence of multiplets, we expect that $3d$ emission from transition-element insulators will appear in a single δ-function line and will provide a "zero-energy" reference (i.e., the energy difference between nearly identical initial and final states) for the photoemission spectrum. Such a reference level is easily identified in the experimental valence-band spectra of Cr_2O_3 shown in Fig. 16(b). The sharp peak at the valence-band edge corresponds to excitation from the (nominally threefold occupied) $3d$ level of the Cr^{3+} ion.[76] Reoccupation of the $3d$ level during measurement means that the $3d$ resonant peak actually provides an approximate measure of the upper valence-band edge (assuming that the $3d$ state fills from levels nearest E_F). That is, with relaxation to a local screening state, photoemission from the $3d$ level only requires enough energy to remove an electron from the valence band.

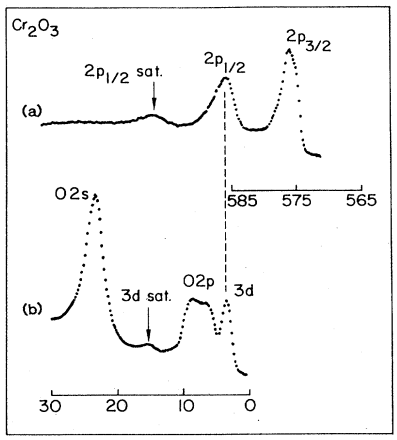

FIG. 16. XPS spectra of (a) Cr $2p$ levels and (b) the valence-band region of Cr_2O_3. The Cr $2p_{1/2}$ and Cr $3d$ peaks are shown in alignment to illustrate that satellite peaks occur at comparable energies from the main line, both at the deep core levels and at the $3d$ level.

This point of view is also supported by molecular cluster calculations of lanthanide trihalides reported by Ruščić *et al.*[77] Mulliken analyses of the transition-state ion (an ion with $\frac{1}{2}$ hole) with the $\frac{1}{2}$ electron removed from a $4f$ level, show an electronic relaxation from ligand orbitals to repopulate the depleted $4f$ shell. Thus the calculated $4f$ removal energy actually represents the removal energy of the least-bound ligand orbital. This, of course, represents a fully relaxed molecular unit, a condition that may not always be probed by photoemission.

Analysis of the XPS valence-band measurement constitutes a problem separate from the analysis of $3d$ emission, requiring examination of the relaxation effects associated with removal of an electron from those valence bands (VB) which are predominately ligand orbitals. To the extent that XPS measures the valence-band ground state, we expect that the locally screened $3d$ peak will appear in coincidence with the upper valence-band edge. In Fig. 16(b), experimental spectra confirm that the $3d$ peak in Cr_2O_3 indeed occurs in coincidence with the upper VB edge.

However, in contradiction to these model predictions, cations ligated to highly electronegative anions show local screening peaks that sometimes occur at anomalously low binding energies. In some compounds, a gap of 1—3 eV may separate the locally screened peak from the valence-band edge.[78,79] Local screening at the cation merely requires the removal of a total charge equal to approximately one electron from the (usually six) ligand near neighbors. However, charge relaxation to compensate for a ligand hole requires a polarization response from second-neighbor ligand atoms. (Near-neighbor cations are ionized and generally will not significantly contribute screening charge.) Thus, ligand screening requires a long-range polarization response mediated by intervening cations. Since this collective response requires such long-range interactions, it may be that the system cannot relax in the time frame of the photoemission experiment. Consequently it is likely that XPS does not monitor a fully relaxed final state at the ligand site but comes much closer at the cation site. This view suggests that, for ligand photoemission, a rather localized final hole state (at the ligand site) is monitored. In contrast, for photoemission from the outermost localized electron shell of cations, the more favorable relaxation conditions permit charge redistribution onto neighboring ligands resulting in the measurement of a more diffuse final hole state. As ligands become less electronegative, the ions become larger, and ligand-ligand overlap increases. For these materials, relaxation of ligand valence-band electrons becomes more favorable following photoemission and the locally screened outer (cation) level appears in closer proximity to the valence-band edge, suggesting that more nearly complete relaxation has occurred.

We now examine the core-level satellite structure of Cr^{3+} compounds using the perspective described in Sec. III (see Fig. 5), considering ground-state configurations ($3d^n4p^{6-n}$). For Cr^{3+}, we regard three of the occupied d electrons to be atomiclike.[80] To represent the nonlocal screening (NLS) condition, then, we use a screening elec-

tron whose orbital makeup is equivalent to the occupied configuration (of the ground state) that is in excess of the three localized d electrons. With this procedure, the NLS can have some $3d$ admixture.[81] This is a somewhat arbitrary procedure for quantifying the nonlocal screening state. The underlying assumption is that the NLS "polarization" state should be reasonably represented by occupation of a low-lying hybridized band that exists separate from minimally hybridized atomiclike $3d$ levels. Calculated results for both screening states at the $2p_{3/2}$ level are shown in Fig. 17.

For Cr_2O_3, the observed separation between local and nonlocal screening peaks at the $2p_{3/2}$ level is 11.1 eV. In Fig. 17 we see that this level separation is obtained from atomic TS calculations for the ground-state configuration $Cr(3d^{3.4}4p^{2.6})$. The calculated energy difference between the locally screened $2p_{3/2}$ and $3d$ levels is 573.9 eV, in close agreement with experiment (573.3 eV). The difference between these experimental and theoretical numbers (0.6 eV) appears in Fig. 17 at the $3d$ level. (In this way, we have measured the $3d$ level using the screened $2p_{3/2}$ core-level peak energies as our point of reference.[82])

For CrF_3, the $2p_{3/2}$ satellite separation increases to 11.8 eV. Again, using Fig. 17, we choose the ground-state configuration that matches the calculated energy difference between local and nonlocal screening states with the experimental satellite separation. The increased separation of CrF_3, relative to Cr_2O_3, indicates a more positive cation potential (that is represented by a configuration with

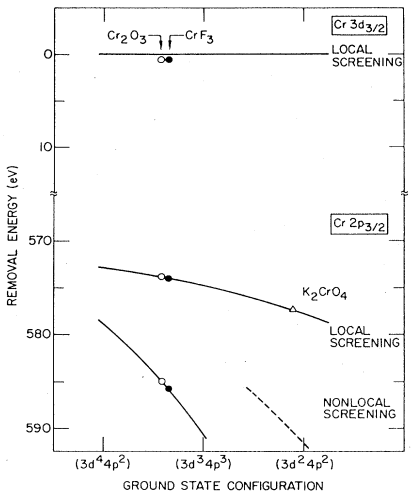

FIG. 17. Calculated (TS) electron-removal energies (solid lines) for $(3d^n4p^{6-n})$ configurations for both local and nonlocal final-state screening conditions. For Cr_2O_3 and CrF_3 the Cr "ground-state configurations" are determined by matching the observed satellite separations with the calculated local-nonlocal energy separations (see text). The potential at the cation site in CrF_3 is seen to be slightly more positive than the corresponding site in Cr_2O_3. After fitting the spectra at the $2p_{3/2}$ level, comparison is made between the measured $3d$ position and the calculated (local screening) $3d$ energy ($E=0$). The Cr "ground-state configuration" is also determined for K_2CrO_4. Here, Cr occurs in the hexavalent state. Satellites are not apparent so the configuration is determined by monitoring the main line (local screening) chemical shift relative to the Cr^{3+} compounds.

slightly reduced $3d$ occupancy). Again we use the $2p_{3/2}$ levels as our point of reference and measure the energy of an electron in the (locally screened) $3d$ level. The difference between the theoretical (574.0 eV) and experimental (573.5 eV) $2p_{3/2}$-$3d$ separations for local screening is 0.5 eV, essentially equivalent to the measurement for Cr_2O_3. Thus for Cr compounds where a reference (zero energy) $3d$ level can be observed, the analytical procedure correctly predicts the trends in the relative level placement that are observed when the local cation potential is varied. Also, remarkably accurate determinations of peak separations, hundreds of eV separated in energy, are obtained from the local-density calculation of the screened hole states.[83]

Using the configuration $(3d^{3.4}4p^{2.6})$ for Cr_2O_3, we now examine the $3d$ shell. The calculated NLS peak occurs at 7.5 eV, with the local screened peak, of course, at 0 eV. A significant prediction of this model picture is the expected occurrence of a NLS satellite peak near the $3d$ peak. Note, in Fig. 16, that the predicted peak is observed. The observed satellite separation at the $3d$ level is slightly greater than the separation at the $2p$'s [Fig. 16(a)], although some reduction in the satellite separation is predicted by the atomic simulation.

This analysis points to another useful insight. Atomic calculations show that the excitation energy needed to remove a localized $3d$ electron, in the absence of extra-atomic relaxation, will be ~ 10 eV or more. This result is experimentally confirmed for free atoms.[84] The free-atom $3d$ removal energies are always significantly greater than $4s$ removal energies.[84] Furthermore, the more highly ionized an atom is, the greater will be the removal energy for occupied localized electrons. For the chemically ionized Cr^{3+} cation characterized by the configuration $3d^{3.4}4p^{2.6}$, the calculated (unscreened) removal energy is 15.8 eV. Thus, the fact that $3d$'s (or other local levels) frequently appear at or near the valence-band edge in ionic compounds is a strong indication that significant extra-atomic relaxation, accompanying photoexcitation, has occurred.

As the Cr valence state is increased to the highly ionized Cr^{6+} condition (as in K_2CrO_4), a substantial increase in the local Cr potential is expected. Charge is drawn from $3d$ levels into molecular orbitals that are rich in O $2p$ character. Unfortunately, core-level satellite features in K_2CrO_4 are apparently too weak and broadened to be discernable from the extrinsic background and, of course, no reference $3d$ peak occurs since all outer electrons participate in molecular orbital formation. However, we suggest that a determination of the Cr core-level chemical shift between Cr_2O_3 and K_2CrO_4 can be obtained by using the O $1s$ line as a fixed energy reference. This procedure appears to be defensible since, with extended x-ray exposure, K_2CrO_4 chemically reduces, leaving superimposed Cr^{6+} and (apparently) Cr^{3+} spectra. While the Cr^{3+} and Cr^{6+} spectra show a large relative chemical shift, the oxygen (and potassium) lines remain unshifted during the reduction process. It seems reasonable, under these circumstances, to infer that the local oxygen potentials for the two compounds are very similar and that relative shifts between Cr^{3+} and Cr^{6+} lines correspond to a change in the local Cr potentials (and not to spurious

charging or band-bending effects, which should affect all core levels in a similar way). Using the O 1*s* as a reference, the chemical shift at the $2p_{3/2}$ peak for K_2CrO_4 relative to Cr_2O_3 is 2.6 eV. This shift is very close to the 2.8-eV binding-energy difference recorded in Ref. 2 for Cr_2O_3 and K_2CrO_4. (However, the usual energy-reference difficulties are encountered with the measurements of Ref. 2.)

Figure 17 would indicate that the final state corresponding to the intense $2p_{3/2}$ peak in K_2CrO_4 must be screened locally. A Cr^{6+} ground-state potential represented by the configuration $(3d^{2.1}4p^{3.9})$ is suggested. For this configuration, a NLS satellite would be expected at ~ 15 eV from the main line. Here the satellite is calculated (dashed line in Fig. 17) with the assumption that the orbital composition of the screening electron is equivalent to the ground-state configuration. (No moment-bearing, localized 3*d* electrons are occupied in K_2CrO_4. Thus no ground-state 3*d* electrons are excluded from the nonlocal screening state as they were in Cr_2O_3.)

F. Satellite structure at the unfilled local shell

We have argued, in Sec. V E, that satellite structure, when apparent at deep core levels, will also be expected in the vicinity of the partially filled, localized outer electron levels. We expect these outer levels to show screening behavior much like that observed at the core levels. We have seen in Fig. 16 that a satellite associated with the $Cr^{3+}(3d^3)$ peak does appear near the valence band of Cr_2O_3.

The 3*d* satellites are predicted for ionic compounds which have occupied atomiclike 3*d* states. If, however, we consider those compounds which are fully ionized (nominal $3d^0$ ions), then we have the remarkable circumstance where strong satellites may be observed following the core levels (since empty 3*d*'s are available for screening) but no satellites can appear adjacent to the valence band. An example of this situation is illustrated in Fig. 18 for ScF_3. Very intense satellites follow the Sc 2*p* doublet, but no corresponding structure appears near E_F since no atomiclike 3*d* levels are available for ionization. Thus we see that, for insulators with strong cation core-level satellites, corresponding satellite features may or may not occur at the 3*d* level. The ability of the simple screening model to predict their occurrence or absence at the 3*d* level provides additional supporting evidence for its validity.

If the screening picture advocated in this paper is correct, then we should expect, for the 3*d* electrons, to observe $n-1$ final-state multiplet structure[85] *at the satellite position.* The low BE structure overlapping the ligand—*p*-bonding orbitals also very likely contains multiplet features but, in this case, the final states contain the original $3d^n$ electron count.

G. Iron compounds: An estimate of ground-state potentials from XPS spectra

Exploiting the observation that cation deep core satellite separations are highly dependent on the local cation ground-state potential, we suggest that with help from the atomic code an estimate of the potential at the cation site can be made. In Fig. 19 we show separations of the calculated screened peaks for Fe ions as a function of varied ground-state electronic configuration $(3d^n4p^{8-n})$. For the Fe^{2+} ions, we hold a "localized 3*d* count" fixed at 6 (see Sec. V E) and screen (nonlocally) with an electron whose charge distribution is equivalent to that of the remaining electrons while for Fe^{3+}, we fixed a localized 3*d* count at 5. Using the satellite data of Fig. 10 for the Fe compounds, in conjunction with the calculated curves of Fig. 19, we find that Fe^{3+} ligated to fluorine neighbors rests in a potential field represented by the configuration $(3d^{5.8}4p^{2.2})$. The *d* count is 5.8, 0.8 in excess of the nominal Fe^{3+} ion configuration. This excess increases to 0.9 and 1.1 for oxygen and chlorine neighbors, respectively. Similarly for Fe^{2+} ions ligated to fluorine, the excess *d* population is 0.5 over the nominal Fe^{2+} ion value and in-

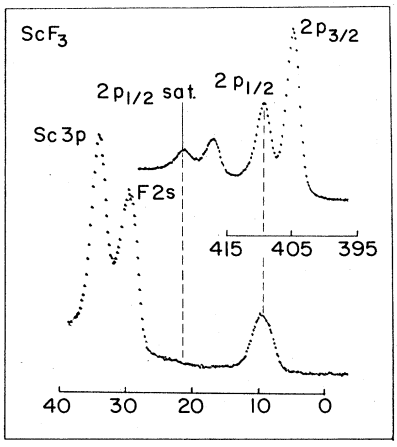

FIG. 18. XPS spectra of Sc 2*p* levels and the valence-band region in ScF_3. Strong satellites follow the 2*p* levels but (unlike Fig. 16) no satellites occur adjacent to the valence bands.

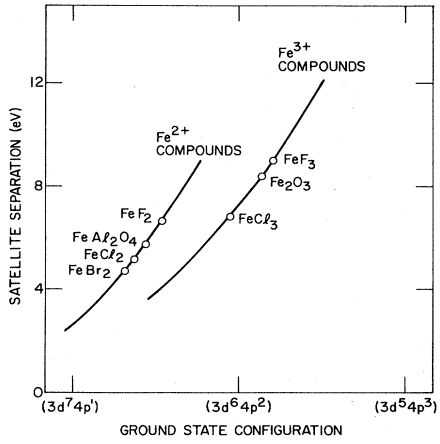

FIG. 19. Calculated (TS) satellite separations (energy difference between local and nonlocal screening of final state) as a function of ground-state configuration for Fe^{2+} and Fe^{3+} cations (solid lines). Experimental satellite energies are used in this figure to estimate the ground-state potential at the cation site.

creases to 0.6, 0.6, and 0.7 for O, Cl, and Br neighbors respectively. Two trends (also noted for the Cr compounds discussed in Sec. V E) are observed:

(1) in a given valence state, the excess d count decreases with increasing ligand electronegativity (charge is more effectively pulled away by the more chemically active ion) and

(2) for a given ligand, the excess d count increases with increasing cation valence state. Both of these trends are generally observed in Mulliken analyses of clusters or solids.

We have pointed out that the nonlocal screening electron wave function is somewhat arbitrarily specified. And, of course, uncertainty regarding this screening state will be translated into a corresponding uncertainty in the deduced ground-state configuration. Thus, while we can readily monitor chemical trends involving charge redistribution, we cannot uniquely measure the ground-state potential. However, a more precise determination of the screening states, possibly by applying molecular-cluster theory, in conjunction with the measured XPS satellite separations, should provide the capability for obtaining an accurate ground-state description of ionic solids. Also, it might provide a basis for extracting, in a straightforward way (as demonstrated above, perhaps), a good approximation to the ground-state potential directly from measurements of XPS satellite separations.

H. Lanthanides

For XPS spectra of lanthanide compounds, the location of $4f$-derived features relative to E_F provides an important clue regarding the nature of the final-state screening conditions. For light lanthanides, it appears that both local and nonlocal screening of deep hole states occur with comparable probabilities. Strong satellites commonly occur at the core levels of La and Ce compounds[31–37] and the $4f$ peak of Ce^{3+} insulators appears near the valence-band edge.[78] However, for compounds of heavier lanthanides ($Z > \sim 63$), it appears that local screening is not observed. In consequence, for the heavy lanthanides, $4f$ spectra generally occur well away from E_F (see Sec. V E) and the complex but well-understood $4f$ multiplet structures measure the $4f$ occupancy of the $n-1$ final state.[85] Since screening for the heavy lanthanides is apparently nonlocal, chemical shifts are large, as confirmed, for example, by observation of large chemical shifts in mixed-valence compounds.[86] SmB_6 shows a chemical shift of ~ 10 eV between core levels (centroids) in the 2+ state relative to the 3+ state.[87]

An even more dramatic feature of light lanthanide systems (which display both screening conditions) results from the fact that local screening should occur via $4f$ electrons which are more localized than the $5s$ and $5p$ core states. Thus the satellite structures associated with the $n=5$ core levels are profoundly different from the satellites associated with the deep core levels. Analysis of these materials, including La^{3+}, Ce^{3+}, and Ce^{4+} insulators, will be the subject of a subsequent paper.

I. Photoemission from ligands

Applying the $Z+1$ analogy to core-level photoemission from ligands leads to rather different considerations from those appropriate for the cation. The very electronegative ligands (e.g., from group VIA and VIIA) in ionic compounds are characterized by a single valence state and nominally have chemically filled shells. For these atoms, advancing from Z to $Z+1$ always involves a valence change of one unit and, nominally, no change in the population of the outermost electron shell. Thus, the outer electron levels of O^{2-} (with an O $1s$ hole) in an ionic compound should reasonably approximate the outer F^{1-} levels. (Recall that addition of a deep hole approximates the addition of a proton.) Consistent with this observation, the ionic radii of O^{2-} and F^{1-} are 1.40 and 1.36 Å, respectively.[88] This very similar ionic size (with a slight contraction for the monovalent species) is characteristic of 2− ions in group VIA and their 1− neighbors in group VIIA. Thus, unlike the case for cation core levels, we would not expect to observe extra-atomic relaxation involving the population of additional orbitals when a ligand deep core hole is created. The ion always has a chemically filled shell. Of course, on a less dramatic scale, an extra-atomic relaxation response will occur since the chemically filled shell of a ligand (of charge Z) is not equivalent to the chemically filled shell of its adjacent (charge $Z+1$) neighbor. Some contraction of the outer p-shell orbitals occurs when the nuclear charge is increased (or a core hole is induced).

Since anion relaxation effects would generally appear to be small, we expect that the energies of ligand XPS peaks should be relatively sensitive to changes in the ground-state local anion potential. When anion shifts are small (apparently the usual case for binary metal-halide compounds when the cation is varied[2,89]), the indication may be that the local halide potential is relatively the same in the different compounds. Because satellite structure associated with local screening states is absent at the ligand core levels, however, chemical information cannot be extracted from the internal level structure in the straightforward way afforded by the transition-metal cations.

J. Other considerations

It appears that, quite generally, the simple relaxation model discussed above will account for the main lines and dominant satellites in deep core (e.g., $2p$) XPS spectra of $3d$ transition-element insulators. However, there are exceptions, where predicted trends are not observed and where spectra are too complex to be readily explained with the simple model. In general, we expect that, for XPS spectra of $3d$ cations, the fully relaxed state will correspond to a locally screened ion and can be associated with a single XPS peak. [It may not always be true, however, that this fully relaxed state is observable with XPS. For example, as noted above, the local ($4f$) screening state apparently is not observable in compounds of heavy lanthanides. However, we cannot identify $3d$ compounds that show this behavior.] Some structure within the locally screened state might be contributed by multiplet excitations. One might expect, however, that cation satellite

spectra could represent a complex assortment of excitations (with a complex photoemission spectrum) rather than a single semirelaxed hole state characterized by nonlocal or band-type screening. For the simpler (e.g., binary ionic) compounds, such spectral complexity appears to be more the exception than the rule. Typically a single strong satellite peak is observed. However, for compounds of copper and nickel, substantially greater spectral complexity is observed. Cation spectra for nickel halides often show two or more satellites.[9,20,25] The main line and first (lowest BE) satellite show behavior that is consistent with the trends predicted by the simple relaxation model discussed above with $3d$ screening accounting for the intense peak.[90] However, at least one additional satellite appears in the heavier nickel halides and shows a separation from the main line that *decreases* with increasing ligand electronegativity. This would appear to be an excitation of common origin for all the Ni halides. (For NiF_2, only a single satellite is apparent, probably because the first and second satellites have merged.) For NiO, a still more complex spectrum is observed.[91] Even the main peak is split into components separated by 1.8 eV.

For divalent copper compounds, predictions of the screening model appear to be quite inappropriate. Satellites are generally composite, varying significantly between the $2p_{1/2}$ and $2p_{3/2}$ peaks and showing a generally decreasing satellite separation with increasing ligand electronegativity.[25] With the apparent strong tendency for local screening to occur in the $3d$-series compounds, it seems likely that the main line corresponds to the fully relaxed, locally screened peak (a conclusion also reached by Ref. 24). The rather general systematics for halides in Fig. 6 also favor this conclusion. However, satellites in the Cu^{2+} compounds appear to be too complex to be described by a single relaxation state.

VI. SUMMARY

We have utilized a relaxation model to account for XPS core-level binding energies and for the energies of prominent satellites that occur in compounds of transition-series elements. For purposes of this paper, illustrative examples have been confined to the first long series ($3d$ elements), but the concepts are also appropriate for the $4d$- and $5d$-series compounds as well as for lanthanides (especially the light elements) and actinides. The occurrence of spectral features (main line and satellite) is attributed to the presence of multiple screening conditions of the photoinduced hole. The nature of the screening electrons and the ground-state potential determines the separation of the satellite from the main line. Below we summarize a number of considerations, discussed in the text, that are relevant to deep core photoionization and to the relaxation model.

a. Intra-atomic relaxation. Intra-atomic relaxation is always associated with the production of a core hole. It is particularly important when electrons in localized orbitals are photoejected since their removal results in substantial reorientation of spectator levels involving large relaxation energies.

b. Extra-atomic relaxation. The production of a core hole leaves an unbalanced nuclear charge at the ion site. This increased positive charge pulls the electron levels of the ion to higher binding energy. It is now energetically favorable for valence electron charge to be attracted from neighboring atoms into the local potential well to screen the core hole.

c. Character of screening orbitals. We expect that transition-metal insulators will contain empty d states that are minimally hybridized (having essentially atomic-like character) as well as radially extended band states. Either type of state may serve to screen the core hole. Occupation of extended-state wave functions is traditionally viewed as a polarization response of the medium to the presence of the local "impurity."

d. The $Z+1$ approximation. For a cation (of atomic number Z) with a deep core hole, a reasonably precise description of the electron states should be provided by representing the ion as a $Z+1$ impurity in the solid. To outer electron levels, the highly localized core hole appears much like a proton added to the cation nucleus. Generally, in going from the Z to $Z+1$ atom, a d electron (in transition-series compounds) is added. Similarly the minimum energy state (fully relaxed state) of the ion involves the occupation of an additional d electron. This represents the local-screening condition. Thus screening by filling a spatially localized orbital generally represents a larger deexcitation energy than screening with an extended orbital (an excited-state condition of the ion).

e. Energetics—implications in XPS spectra. Since screening involves a deexcitation process, the kinetic energy of the photoelectron will be enhanced (by the screening process) and the apparent XPS binding energy of the screened state will thus be reduced relative to the XPS binding energy of the unscreened core hole. The low-binding-energy intense XPS line thus corresponds to a more fully relaxed condition than does the satellite. This interpretation is consistent with a shakeup picture if we regard the main line as fully relaxed (i.e., locally screened) with the satellite being an excitation *relative to this fully relaxed state.*

f. Temporal considerations. If multiple screening possibilities are observable, then time scales in the photoemission process must play a fundamentally important role. Clearly, there is only one "ground-state" screening condition. That is, if the core hole is sufficiently long lived, only orbitals for the least energetic of the possible screening states will eventually become occupied to screen the core hole. Thus, nonlocal screening states, to be observable as sharp satellites, must have lifetimes of at least $\sim 10^{-16}$ sec, the photoemission lifetime. The coupling between those extended and local states of the cation determine the electron residence time in the extended screening states.

g. Chemical shifts. The preceding analysis has shown why chemical shifts (involving the main line) are generally small for transition-element compounds, even when large cation valence changes are involved. The small shifts are a consequence of local screening of the core hole, a relaxation process which minimizes chemical sensitivity in XPS spectra. Greater chemical sensitivity is found at the satellite. Consequently, the *relative spacing* of local and nonlo-

cal screening peaks (XPS main line and satellite) associated with the cation is sensitive to the cation ground-state chemical environment. The peak separation increases as electron charge is pulled away from cation site. Thus we argue that chemical-bonding information, including cation valence state, can be obtained from measurements of the satellite separation relative to the main line. Unlike traditional measurements of absolute binding-energy shifts for studying chemistry, this approach does not require the determination of an energy reference (an unsatisfactorily resolved problem for insulating materials).

VII. CONCLUSIONS

In this paper, we have, with several case studies, sought to demonstrate that the intense, low-binding-energy peak associated with XPS core-level photoemission measures, for $3d$ transition-element insulators, the energy difference between the ground state of the insulator and a final ion state where the core hole is compensated by occupation of an outer $3d$ electron acquired from surrounding ligand orbitals. This viewpoint is supported by (fully relaxed) self-consistent field (SCF) calculations of ground-state and hole-state molecules,[77] clusters,[62,92] or "supercells,"[93] where population analyses of the ground state and hole state consistently show that the core hole is predominately compensated by a $3d$ (or, for lanthanides, a $4f$) electron. Thus, while energetics considerations generally support the local-screening interpretation of the intense peak, XPS measurement time considerations could, in principle, exclude it. The systematic studies reported in this paper support the view that the local-screening description is generally appropriate for the final core-hole state associated with the intense peak in $3d$ insulators. (This condition is apparently not so generally true for lanthanide compounds.) It then follows that the (higher BE) satellites are associated with states of the system which are not fully relaxed. Core-hole screening (still a relaxation response) could occur by partial electron occupation of spatially extended band states which lie above the localized $3d$'s. The result is a single, many-electron polarization state centered at the impurity site. This simple model view, with guidance from atomic calculations and simulated local-cation potentials, appears to provide substantial predictive capability. Observed satellite separations for simple compounds are correlated with cation valence states and with anion and cation electronegativities.

To test these model ideas more quantitatively, the satellite separation from the main line will be calculated for a model cluster using transition-state theory, by considering (1) the fully relaxed (core-hole) ion state to obtain the locally screened main line and (2) by performing a second SCF calculation, while preventing compensating population of localized $3d$ orbitals, to obtain the satellite.[92] In this view, the dominant charge flow response to core-electron ejection is electron migration from ligands toward the core hole, both for the main line and for the satellite.

ACKNOWLEDGMENTS

The authors are grateful to numerous people for participating in valuable and stimulating discussions pertaining to the work presented here. Deserving special mention are the contributions of D. J. Lam, D. E. Ellis, A. J. Freeman, D. D. Koelling, M. Norman, and S. Bader. We are also grateful to J. W. Stout for providing samples of $FeCl_2$ (ingot) and $FeCl_3$, and to N. L. Peterson for supplying an ingot of Cr_2O_3. This work was supported by the U.S. Department of Energy.

[1]K. Siegbahn, C. Nordling, A. Fahlman, R. Nordberg, A. Hamrin, J. Hedman, G. Johansson, T. Bergmark, S. Karlson, I. Lindgren, and B. Lindberg, Nova Acta Regiae Soc. Sci. Ups. (Sec. IV) **20**, 1 (1967).

[2]C. D. Wagner, W. M. Riggs, L. E. Davis, and J. F. Moulder, in *Handbook of X-Ray Photoelectron Spectroscopy,* edited by G. E. Muilenberg (Perkin Elmer Corporation, Eden Prairie, Minn., 1979).

[3]C. Fadley, in *Electron Emission Spectroscopy,* edited by W. Dekeyser, L. Fiermans, G. Vanderkelen, and J. Vennik (Reidel, Boston, 1973), p. 151.

[4]A. Rosencwaig, G. K. Wertheim, and H. J. Guggenheim, Phys. Rev. **27**, 479 (1971).

[5]G. K. Wertheim and S. Hufner, Phys. Rev. Lett. **28**, 1028 (1972).

[6]A. Rosencwaig and G. K. Wertheim, J. Electron Spectrosc. Relat. Phenom. **1**, 493 (1973).

[7]T. A. Carlson, J. C. Carver, L. J. Saethre, F. Garcia Santibáñez, and G. A. Vernon, J. Electron Spectrosc. Relat. Phenom. **5**, 247 (1974).

[8]T. A. Carlson, J. C. Carver, and G. A. Vernon, J. Chem. Phys. **62**, 932 (1975).

[9]G. A. Vernon, G. Stucky, and T. A. Carlson, Inorg. Chem. **15**, 278 (1976).

[10]T. Novakov and R. Prins, Solid State Commun. **9**, 1975 (1972).

[11]T. Novakov, Phys. Rev. B **3**, 2693 (1971).

[12]T. Novakov and R. Prins, in *Electron Spectroscopy,* edited by D. A. Shirley (North-Holland, Amsterdam, 1972), p. 821.

[13]B. Wallbank, I. G. Main, and C. E. Johnson, J. Electron Spectrosc. Relat. Phenom. **5**, 259 (1974).

[14]B. Wallbank, C. E. Johnson, and I. G. Main, J. Phys. C **6**, L340 (1973).

[15]D. C. Frost, A. Ishitani, and C. A. McDowell, Mol. Phys. **24**, 861 (1972).

[16]D. C. Frost, C. A. McDowell, I. S. Woolsey, Chem. Phys. Lett. **17**, 320 (1972).

[17]D. C. Frost, C. A. McDowell, and B. Wallbank, Chem. Phys. Lett. **40**, 189 (1976).

[18]B. Wallbank, J. S. H. Q. Perera, D. C. Frost, and C. A. McDowell, J. Chem. Phys. **69**, 5405 (1978).

[19]J. S. H. Q. Perera, D. C. Frost, and C. A. McDowell, J. Chem. Phys. **72**, 5151 (1980).

[20]L. J. Matienzo, L. I. Yin, S. O. Grim, and W. E. Swartz, Inorg. Chem. **12**, 2762 (1973).

[21]I. Ikemoto, K. Ishii, H. Kuroda, and J. M. Thomas, Chem. Phys. Lett. **28**, 55 (1974).

[22]K. S. Kim, Phys. Rev. B **11**, 2177 (1975).

[23]K. S. Kim and N. Winograd, Chem. Phys. Lett. **31**, 312 (1975).

[24]G. Van der Laan, C. Westra, C. Haas, and G. A. Sawatzky, Phys. Rev. B **23**, 4369 (1981).
[25]G. A. Sawatzky, in *Studies in Inorganic Chemistry,* edited by R. Metselaar, H. J. M. Heijligers, and J. Shoonman (Elsevier, Amsterdam, 1983), Vol. 3, p. 3.
[26]M. Brisk and A. D. Baker, J. Electron Spectrosc. Relat. Phenom. **6**, 81 (1975).
[27]S. K. Sen, J. Riga, and J. Verbist, Chem. Phys. Lett. **39**, 560 (1976).
[28]M. Scrocco, J. Electron Spectrosc. Relat. Phenom. **19**, 311 (1980).
[29]H. Chermette, P. Pertosa, and F. M. Michel-Calendini, Chem. Phys. Lett. **69**, 240 (1980).
[30]J. K. Gimzewski, D. J. Fabian, L. M. Watson, and S. Affrossman, J. Phys. F **7**, L305 (1977).
[31]G. K. Wertheim, R. L. Cohen, A. Rosencwaig, and H. J. Guggenheim, in *Electron Spectroscopy,* edited by D. A. Shirley (North-Holland, Amsterdam, 1972), p. 813.
[32]A. J. Signorelli and R. G. Hayes, Phys. Rev. B **8**, 81 (1973).
[33]S. Suzuki, T. Ishii, and T. Sagawa, J. Phys. Soc. Jpn. **37**, 1334 (1974).
[34]C. K. Jorgensen and H. Berthou, Chem. Phys. Lett. **13**, 186 (1972).
[35]H. Berthou, C. K. Jorgensen, and C. Bonnelle, Chem. Phys. Lett. **38**, 199 (1976).
[36]C. K. Jorgensen, Struct. Bonding (Berlin) **24**, 1 (1975).
[37]P. Burroughs, A. Hamnett, A. Orchard, and G. Thornton, J. Chem. Soc. Dalton Trans. 1686 (1976).
[38]J. J. Pireaux, J. Riga, E. Thibaut, C. Tenret-Noel, R. Caudano, and J. J. Verbist, Chem. Phys. **22**, 113 (1977).
[39]B. W. Veal, D. J. Lam, H. Diamond, and H. R. Hoekstra, Phys. Rev. B **15**, 2929 (1977).
[40]C. Keller and C. K. Jorgensen, Chem. Phys. Lett. **32**, 397 (1975).
[41]R. J. Thorn, J. Phys. Chem. Solids **43**, 571 (1982).
[42]Wei-Yean Howng and R. J. Thorn, Chem. Phys. Lett. **56**, 463 (1978).
[43]G. Michael Bancroft, Tsun K. Sham, and Sven Larsson, Chem. Phys. Lett. **46**, 551 (1977).
[44]G. C. Allen, J. A. Crofts, M. T. Curtis, P. M. Tucker, D. Chadwick, and P. Hampson, J. Chem. Soc. Dalton Trans. 1296 (1974).
[45]See, for example, C. S. Fadley, in *Electron Spectroscopy: Theory, Techniques, and Applications,* edited by C. R. Brundle and A. D. Baker (Academic, New York, 1978), Vol. 2, p. 2.
[46]See Rashmi-Rekha, Satya Pal, and R. P. Gupta, Phys. Rev. B **26**, 35 (1982) and references therein.
[47]S. Larsson, Chem. Phys. Lett. **40**, 362 (1976); S. Larsson and M. Braga, *ibid.* **48**, 596 (1977).
[48]J. C. Fuggle, M. Campagna, Z. Zolnierek, R. Lässer, and A. Platau, Phys. Rev. Lett. **45**, 1597 (1980).
[49]B. W. Veal and A. P. Paulikas, Phys. Rev. Lett. **51**, 1995 (1983).
[50]L. Ley, S. P. Kowalczyk, F. R. McFeely, R. A. Pollak, and D. A. Shirely, Phys. Rev. B **8**, 2392 (1973); D. A. Shirley, R. L. Martin, S. P. Kowalczyk, F. R. McFeely, and L. Ley, *ibid.* **15**, 544 (1977).
[51]R. L. Martin and D. A. Shirley, in *Electron Spectroscopy, Theory, Techniques, and Applications,* edited by C. R. Brundle and A. D. Baker (Academic, New York, 1977), p. 75.
[52]S. P. Kowalczyk, L. Ley, F. R. McFeely, R. A. Pollak, and D. A. Shirley, Phys. Rev. B **9**, 381 (1974).
[53]A. Kotani and Y. Toyazawa, Jpn. J. Phys. **35**, 1073 (1973); **35**, 1082 (1973); **37**, 912 (1974); A. Kotani, *ibid.* **46**, 488 (1979).
[54]R. Hoogewijs, L. Fiermans, and J. Vennik, Surf. Sci. **69**, 273 (1977).
[55]N. D. Lang and A. R. Williams, Phys. Rev. B **16**, 2408 (1977).
[56]K. Schönhammer and O. Gunnarsson, Solid State Commun. **23**, 691 (1977); Z. Phys. B **30**, 297 (1980).
[57]J. C. Fuggle, E. Umbach, D. Menzel, K. Wandelt, and C. R. Brundle, Solid State Commun. **27**, 65 (1978); J. C. Fuggle, F. U. Hillebrecht, Z. Zolnierek, R. Lässer, Ch. Freeburg, O. Gunnarsson, and K. Schönhammer, Phys. Rev. B **27**, 7330 (1983); J. C. Fuggle, in *X-Ray and Atomic Inner-Shell Physics—1982 (International Conference, University of Oregon),* edited by Bernd Craseman (AIP, New York, 1982), p. 661.
[58]P. S. Bagus and K. Hermann, Surf. Sci. **89**, 588 (1979); K. Hermann and P. S. Bagus, Solid State Commun. **38**, 1257 (1981).
[59]B. Johansson and N. Mårtensson, Phys. Rev. B **21**, 4427 (1980); **24**, 4484 (1981); B. Johansson, *ibid.* **30**, 3533 (1984).
[60]In general, the wave-function composition of the charge compensating or screening orbitals will not be identical to the nominally equivalent orbitals of the ground state atom.
[61]SCF calculations of transition-element molecules or clusters which include a $3d$ or deep core hole show that the hole becomes screened by occupation of a $3d$ orbital. See, for example, J. A. Tossell, J. Electron Spectrosc. Relat. Phenom. **8**, 1 (1976).
[62]O. Gunnarsson and K. Schönhammer, Phys. Rev. B **22**, 3710 (1980).
[63]See, for example, M. Cardona and L. Ley, *Photoemission in Solids I,* Vol. 26 of *Topics in Applied Physics,* edited by M. Cardona and L. Ley (Springer, Berlin, 1978), p. 1.
[64]P. H. Citrin and T. D. Thomas, J. Chem. Phys. **57**, 4446 (1972).
[65]Fuggle *et al.* (Ref. 48) have used the terminology "well screened" and "poorly screened" to describe these final-state conditions. The well-screened state corresponds to occupancy of a localized charge-compensating electron orbital.
[66]M. A. Brisk and A. D. Baker, J. Electron Spectrosc. Relat. Phenom. **7**, 197 (1975).
[67]G. Wendin, Struct. Bonding (Berlin) **45**, 1 (1981).
[68]This code was originally developed by D. A. Liberman, D. T. Cromer, and J. T. Waber, Phys. Rev. **137**, 27 (1965). Subsequently, the code was extensively revised and simplified by D. D. Koelling. We are grateful to Dr. Koelling for making the revised code available to us. For all calculations reported here, const $\propto \rho^{1/3}$ exchange was used. ρ is the charge density and the coefficient α was set equal to $\frac{2}{3}$.
[69]J. C. Slater, *The Self-Consistent Field for Molecules and Solids,* Vol. 4 of *Quantum Theory of Molecules and Solids* (McGraw-Hill, New York, 1974).
[70]This point has been well recognized in the literature. See for example, E. H. S. Burhop, *The Auger Effect* (Cambridge University Press, Cambridge, 1952), and Ref. 59 for an extensive discussion.
[71]The possibility of chemical sensitivity in satellite separations has been considered by other researchers, usually within the framework of a model that associates the satellite with a shakeup process. For example, see Ref. 36.
[72]A peak appears in the Fe^{3+} spectra at 15—18 eV from the $2p_{1/2}$ peak. However, we do not believe the peak results from a nonlocal screening relaxation response to photoejection and thus have not displayed the feature in Fig. 9.
[73]L. Pauling, *The Nature of the Chemical Bond* (Cornell Univer-

sity Press, Ithaca, 1960).

[74]I. Ikemoto, K. Ishii, S. Kinoshita, T. Fujikawa, and H. Kuroda, Chem. Phys. Lett. **38**, 467 (1976).

[75]I. Ikemoto, K. Ishii, S. Kinoshita, and H. Kuroda, J. Electron Spectrosc. Relat. Phenom. **11**, 251 (1977).

[76]See, for example, D. E. Eastman and J. L. Freeouf, Phys. Rev. Lett. **34**, 395 (1975).

[77]B. Ruščić, G. Goodman, and J. Berkowitz, J. Chem. Phys. **78**, 5443 (1983), and private communication.

[78]S. Sato, Y. Sakisaka, and T. Matsukawa, *Vacuum Ultraviolet Radiation Physics,* edited by E. Koch, R. Haensel, and C. Kunz (Pergamon, Vieweg, 1974), p. 414.

[79]J. M. Dyke, N. K. Fayad, A. Morris, I. R. Trickle, and G. C. Allen, J. Chem. Phys. **72**, 3822 (1980).

[80]D. Adler, *Insulating and Metallic States in Transition Metal Oxides,* Vol. 21 of *Solid State Physics,* edited by H. Ehrenreich, Frederick Seitz, and David Turnbull (Academic, New York, 1968), p. 1.

[81]For example, the transition-state energy for removal of a Cr $2p_{3/2}$ electron that experiences nonlocal screening, from an environment where the Cr ground-state potential is represented by $Cr(3d^4 4p^2)$, is obtained from the SCF calculation of $Cr(2p_{3/2}^{3.5})(3d^4 4p^2)(3d^{0.165} 4p^{0.335})$. The removal energy E_{exc} is given by $E_{exc} = -E_{2p_{3/2}} + 0.33E_{3d} + 0.67E_{4p}$, where $E_{2p_{3/2}}$, E_{3d}, and E_{4p} are eigenvalues from the atomic calculation (see Sec. III).

[82]Reference 2 lists a binding energy of 576.6 eV for the $2p_{3/2}$ peak using conventional calibration procedures.

[83]Electron-removal energies for deep core levels are quite sensitive to the exchange coefficient α. A small adjustment of α would make these energy differences agree with experiment.

[84]K. D. Sevier, At. Data Nucl. Data Tables **24**, 323 (1979).

[85]G. K. Wertheim, in *Electron Spectroscopy: Theory, Techniques, and Applications,* edited by C. R. Brundle and A. D. Baker (Academic, New York, 1978), Vol. 3, p. 259.

[86]M. Campagna, G. K. Wertheim, and E. Bucher, Struct. Bonding (Berlin) **30**, 99 (1976).

[87]J.-N. Chazalviel, M. Campagna, G. K. Wertheim, and P. H. Schmidt, Solid State Commun. **19**, 725 (1976).

[88]R. D. Shannon, Acta Crystallogr. Sect. A **32**, 751 (1976).

[89]R. G. Hayes and N. Edelstein, in *Electron Spectroscopy,* edited by D. A. Shirley (North-Holland, Amsterdam, 1972), p. 771.

[90]This description of the main peak was also offered by A. Fujimori, F. Minami, and S. Sugano, Phys. Rev. B **29**, 5255 (1984).

[91]S. Hüfner and G. K. Wertheim, Phys. Rev. B **8**, 4857 (1973).

[92]B. W. Veal, D. J. Lam, and D. E. Ellis (unpublished).

[93]M. Norman, D. D. Koelling, and A. J. Freeman (private communication).